INTERNATIONAL JOURNAL OF PRECISION ENGINEERING AND MANUFACTURING Vol. 19, No. 10, pp. 1507-1513 OCTOBER 2018 / 1507

REGULAR PAPER

DOI: 10.1007/s12541-018-0177-x
ISSN 2234-7593 (Print) / 2005-4602 (Online)

Development of Efficiency Enhanced Scotch Yoke Mechanism for Robotic Fish

Seok-Ryung Kwon[1], Dae-Young Lee[2], Useok Jeong[3], Yong-Jai Park[4,#], and Kyu-Jin Cho[2,#]

1 Advanced Gasoline Engine Development Team, Hyundai Motor Company, 150, Hyundaiyeonguso-ro, Namyang-eup, Hwaseong-si, Gyeonggi-do, 18280, Republic of Korea
2 School of Mechanical and Aerospace Engineering/SNU-IAMD, Seoul National University, 1 Gwanak-ro, Gwanak-gu, Seoul, 08826, Republic of Korea
3 Robot R&D Group, Korea Institute of Industrial Technology, A143, Hanggaul-ro, Sangnok-gu, Ansan-si, Gyeonggi-do, 15588, Republic of Korea
4 Department of Mechatronics, Kangwon National University, 1, Gangwondaehak-gil, Chuncheon-si, Gangwon-do, 24341, Republic of Korea
Corresponding Authors / E-mail: yjpark@kangwon.ac.kr, TEL: +82-33-250-6371, ORCID: 0000-0002-8830-3270
E-mail: kjcho@snu.ac.kr, TEL: +82-2-880-1663, ORCID: 0000-0003-2555-5048

KEYWORDS: Scotch yoke mechanism, Robotic fish, Propulsion system, Torque distribution

A Scotch yoke mechanism can provide high thrust by generating high frequency flapping motion in a propulsion system of robotic fish. However, higher frequency makes higher drag force, and if the motor torque is insufficient compared to the drag force, this causes a lagging phenomenon due to the lack of torque, which causes a problem of lowering the thrust. In this paper, we propose an efficiency enhanced scotch yoke mechanism through output torque re-distribution. We focus on the fact that the required motor torque of the Scotch yoke mechanism is not constant in the fin propulsion system; thus, it is not necessary to raise the torque in the entire domain. By transferring the extra torque in a certain section to the torque-insufficient section, the frequency and thrust can be increased without increasing the motor size and energy consumption. We present a dynamic model and a design method of the proposed concept, and also validate the performance enhancement by comparing the thrust, frequency, and the period of the tail fin movement of conventional and enhanced system while the equal input current is supplied.

Manuscript received: January 18, 2018 / Revised: July 8, 2018 / Accepted: July 13, 2018

NOMENCLATURE

r = Radius of the crank wheel pin
R = Length of the link
l = Radius of gear
p_{Rack} = Position of the rack
ω = Angular speed of the motor
v_{Rack} = Velocity of the rack
$v_{Tail\,fin}$ = Velocity of the tail fin
F_d = Drag force toward the tail fin
F_r = Force that acts on the motor
τ_m = Motor torque
τ_r = Required torque
R_C = Radius of the crank wheel
r_{rol} = Radius of the roller
B = Desired torque amplitude
α = Slope angle of the crank wheel surface
k = Spring constant
h = Height of the path of the roller
h' = Compensated height of the path of the roller
θ = Phase angle
θ' = Compensated phase angle
F_k = Compressive force on the crank wheel
F_T = Torsional force on the crank wheel

1. Introduction

In robotics, there has been a growing interest in bio-inspired robotic fish for exploring sea and for collecting resources. Specifically, the biomimetic propulsion system provides better power efficiency and maneuverability than the conventional propeller propulsion system.[1] In general, most studies on the robotic fish proposed more efficient swimming performance.[2-9] Low et al. conducted an experiment to investigate the swimming performance of a robotic fish using various design parameters.[10] They showed that the frequency and amplitude

were important parameters for the thrust of the robotic fish. However, it is difficult for a robotic fish that uses a servomotor to generate a high frequency due to lack of the proper amount of torque and velocity. To cope with this phenomenon, some researchers have tried to use the Scotch yoke mechanism with a direct current (DC) motor for a robotic fish.[11-14]

The Scotch yoke mechanism changes the rotation of the motor to reciprocating motion, which is used in various fields.[15-17] In this mechanism, the DC motor can rotate at a constant speed when the tail fin of the robot fish reciprocates. Conversely, in case of the tail fin driven by a servo motor, the angular velocity of servo motor decreases in order to change the direction of movement of the tail fin. Yu et al. designed the RoboDolphin-III, which used a Scotch yoke mechanism and compared its thrust with a robotic fish that used servo motors.[18] This study showed that the robotic fish using the Scotch yoke mechanism operates at a higher frequency than the robotic fish using servo motors. In addition, Park et al. conducted experiments that showed the relationship between thrust and frequency of caudal fin.[19] It was noted that the thrust generally increased as the frequency increased below a specific frequency. However, higher frequency makes higher drag force, and if the motor torque is insufficient compared to the drag force, this causes a lagging phenomenon due to the lack of torque, which causes a problem of lowering the thrust.

In this paper, we propose an efficiency enhanced scotch yoke mechanism through output torque re-distribution to solve this problem. We focus on the fact that the required motor torque of the Scotch yoke mechanism is not constant in the fin propulsion system; thus, it is not necessary to raise the torque in the entire domain. If the torque can be used efficiently by transferring the extra torque in a certain section to the torque-insufficient section, the thrust can be increased without increasing the motor size and energy consumption.

The mechanism uses springs and specially designed crank wheel to customize the output torque at the desired moment. We derive the analytic model that generates the required torque profile and the desired design parameters of the mechanism. To verify the concept, we built the proposed mechanism with the conventional mechanism, and conducted the experiments to confirm the performance in the constrained condition. In addition, the angular position of the tail fin is measured to analyze the behavior of the mechanism. The experimental results show that the proposed Scotch yoke mechanism increases the thrust by 27 percent without increasing the energy consumption.

2. Propulsion System with Scotch Yoke Mechanism

2.1 Characteristics of the Scotch yoke mechanism

This section describes the features of the Scotch yoke mechanism. The Scotch yoke mechanism changes the rotational motion to the reciprocating motion. Thus, this mechanism can use high speed DC motor. This advantage allows the tail fin to flap faster. Fig. 1 shows the movement of the Scotch yoke mechanism. The rotating motion of the crank wheel is translated to an up-and-down motion. Fig. 1 shows the movement of the Scotch yoke mechanism. The rotational motion of the crank wheel is translated to an up-and-down motion.

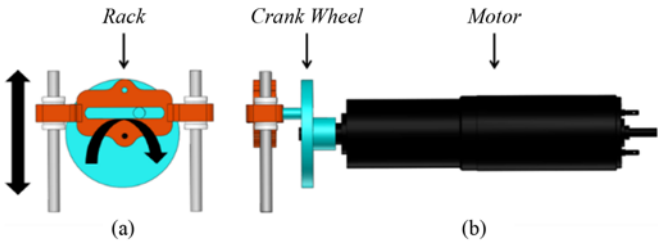

Fig. 1 Overall design of the Scotch yoke mechanism; (a) front view, (b) side view

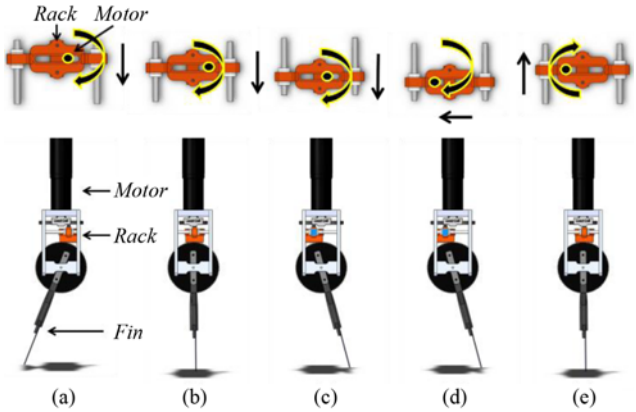

Fig. 2 Schematic drawing of the Scotch yoke mechanism: the top is the motion of the rack, and the bottom is the movement of the tail fin when (a) the rack is in the top, (b) the rack moves to the bottom, (c) rack is in the bottom, (d) the rack changes direction, and (e) the rack moves to the top

Fig. 2 describes the change in the location of the tail fin depending on the movement of the crank wheel. The rack moves up and down while the crank wheel rotates along the ellipsoidal hole of the rack. The gear of the rack spins the round gear that is connected to the tail fin. As a result, the tail fin moves from side to side, while the rack moves up and down. During this process, the drag force is applied to the tail fin and torque is applied to the motor. We defined this torque as the required torque. There are noticeable characteristics about the required torque. The required torque changes while the motor that uses the Scotch yoke mechanism rotates. In particular, the crank wheel moves the rack relatively less when the tail fins change direction of movement. In this process, the required torque is smaller than other conditions. In contrast, the required torque increased when the tail fin approached central part of the section where the tail moves. If the maximum torque of the motor is less than the required torque, the motor does not work properly. Moreover, the angular velocity of the motor is influenced by the torque of the motor. Thus, the movement of the tail fin is affected by the torque of the motor.

Because of this phenomenon, the motor torque is an important factor in the Scotch yoke mechanism. Therefore, we are interested in the method to control the motor torque that influences the movement of the tail fin. Consequently, the features of the Scotch yoke mechanism are analyzed.

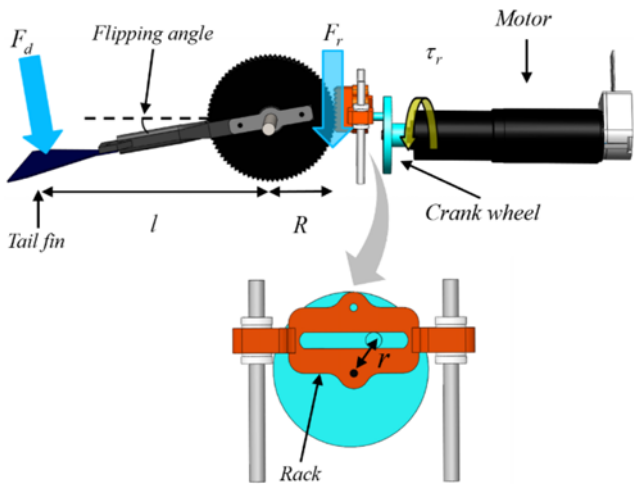

Fig. 3 Parameters for the dynamic model of the Scotch yoke mechanism

2.2 Dynamic model of Scotch yoke mechanism

The exact value of the required torque of the Scotch yoke mechanism is difficult to compute with the analytical model because of its complex fluid dynamic behavior. Since obtaining accurate torque is beyond the scope of this paper, we simplified the problem using general fluid dynamics and estimated the required torque.

The simplified dynamic model for the required torque estimation is driven by the following equations. Fig. 3 presents the parameters for the equation.

Assuming that the shaft of the motor rotates with a constant speed ω, the speed of the tail fin can be calculated as

$$p_{Rack} = r\sin\omega t \tag{1}$$

$$v_{Rack} = r\omega\cos\omega t \tag{2}$$

$$v_{Tail\,fin} = \frac{l}{R}v_{Rack} = \frac{l}{R}r\omega\cos\omega t \tag{3}$$

and, the drag force applied to the tail fin in the direction of the velocity can be calculated as

$$F_d = \frac{1}{2}\rho v_{Tail\,fin}^2 C_d A = \frac{1}{2}\rho C_d A\left\{\frac{l}{R}r\omega\cos(\omega t)\right\}^2 \tag{4}$$

Based on Eq. (4), the applied force to the rack, F_r and the required torque of the motor, τ_r can be calculated as

$$|F_r| = \frac{l}{R}|F_d| = \frac{1}{2}\rho C_d A\left(\frac{l}{R}\right)^3\{r\omega\cos(\omega t)\}^2 \tag{5}$$

$$|\tau_r| = |F_r r\cos(\omega t)| = \frac{1}{2}\rho C_d A\omega^2\left(\frac{l}{R}r\right)^3|\cos^3(\omega t)| \tag{6}$$

From the equations, the required torque of the motor can be expressed in trigonometric function form while the maximum capable torque of the motor is fixed. The results are plotted in Fig. 4 to describe the required torque when the numerical values from Table 1 are used. The required torque is similar to the sinusoidal. The solid line describes the torque generated by the motor and the dotted line shows the required torque. The graph shows that the required torque is larger than the motor torque in certain sections. In this variation, the angular velocity of the motor is decreased because the torque is insufficient. As a result, the frequency of the tail fin does not increase above certain value and the thrust is reduced. Therefore, we stored the motor torque from the area where the required torque is relatively low and released it at the certain moment which needs higher torque to solve an aforementioned problem, as shown in Fig. 4(b).

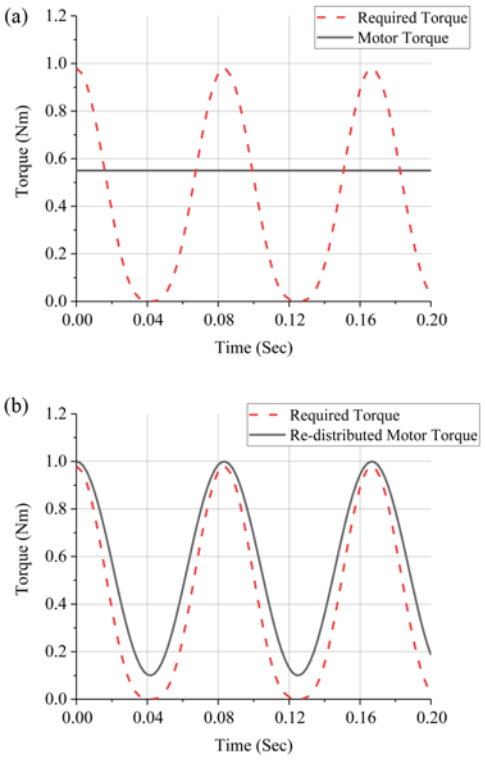

Fig. 4 Comparison between the motor torque and the required torque in specific frequency (6 Hz); (a) Conventional Scotch yoke mechanism, (b) Efficiency enhanced Scotch yoke mechanism

Table 1 Simulation parameters

Density of water (ρ)	1000 kg/m^3
Drag coefficient of a flat plate (C_d)	1.28
Area of fin (A)	4000 × 10^{-6} m^2
Radius of gear (R)	40 × 10^{-3} m
Radius of crank wheel pin (r)	15 × 10^{-3} m
Length of the link (l)	17 × 10^{-2} m

3. The Efficiency Enhanced Scotch Yoke Mechanism

3.1 Design of the efficiency enhanced Scotch yoke mechanism

In order to re-distribute the torque, we propose to use a curve-shape crank with coil springs to store and release the energy. The redundant energy in the low torque required section is stored in the compression coil springs and the stored energy is released in the section requiring high torque. Instead of adding extra parts to compress the springs, we change the shape of the crank wheel that is already being used by the

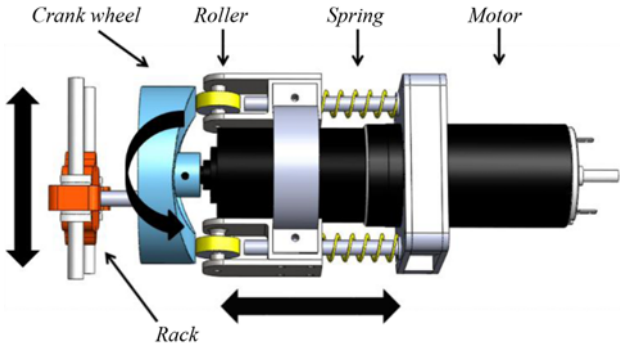

Fig. 5 The components of the efficiency enhanced Scotch yoke mechanism with springs

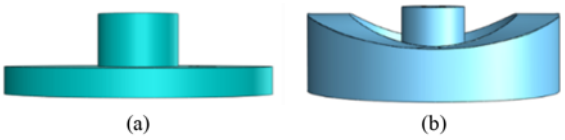

Fig. 6 Crank wheel side view (a) Conventional crank wheel (b) Curved shape crank wheel

Scotch yoke mechanisms to reduce the complexity of the mechanism

Fig. 5 shows the details of the proposed Scotch yoke mechanism which consists of the crank wheel, rollers, and springs. The crank wheel is designed to have a curved shape to push the rollers. The rollers that face the crank wheel move side to side, and the springs are compressed along the rod. In this process, the torque of the motor is stored in the springs. When the motor starts to rotate, the contact point changes according to the surface of the crank wheel because the crank wheel is designed as the curved shape to produce the sinusoidal torque graph. The output torque of the motor is changed by this mechanism, while the rollers move along the surface of the crank wheel from side to side. After the released torque from the springs is added to the maximum capable torque, the final torque of the motor can be higher than the required torque. As a result, we obtain similar torque profile with the required torque using this mechanism.

In the newly designed mechanism, specifically, the difference between the conventional design and the new design is the shape of the crank wheel. In the curved shape crank wheel as shown in Fig. 6, the rollers move along the surface in parallel with the axis of the motor. In addition, this shape is determined by the maximum capable torque of the motor. The design of the crank wheel will be explained precisely in the next chapter.

3.2 Design of the crank wheel

The height of the crank wheel surface determines the compression displacement of the spring, and the slope determines the ratio between the compressive force and the torsional force as shown in Fig. 7. Therefore, the desired torque profile can be achieved by designing the height and the slope according to a specific phase angle.

The required torque from Eq. (6) has complex periodic form. Instead of following the function exactly, we mimic the target profile by using a sum of constant motor torque and a simple trigonometric function

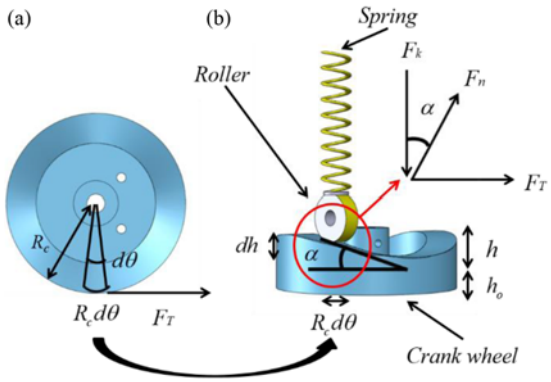

Fig. 7 Free body diagram of the crank wheel; (a) Front view, (b) Side view

with equal frequency as in Eq. (7).

$$\frac{1}{2}\rho C_d A \omega^2 \left(\frac{l}{R} r\right)^3 \left|\cos^3\theta\right| \approx \tau_m + B\cos 2\theta \tag{7}$$

In summary, the surface shape of the crank wheel needs to generate the torque with desired trigonometric form, and it can be derived as follows.

The slope angle, α determines the force ratio between the compressive force and the torsional force.

$$\tan\alpha = \frac{dh}{R_C d\theta} = \frac{F_T}{F_k} \tag{8}$$

And each force can be presented as

$$F_T R_C = B\cos 2\theta \tag{9}$$

$$F_k = k(h - h_0) \tag{10}$$

From Eqs. (8)-(10), it possible to derive a equation which represent the relationship between θ and h.

$$k(h - h_0)dh = B\cos 2\theta \quad d\theta \tag{11}$$

$$h^2 - 2h_o h - \frac{B}{k}\sin 2\theta = 0 \tag{12}$$

$$h = h_0 + \sqrt{h_0^2 + \frac{B}{k}\sin 2\theta} \tag{13}$$

We neglect the frictional force between the rollers and the crank wheel, since the friction coefficient is relatively small.

If the diameter of the roller is not negligibly small, this will cause the shift of the height and the phase angle of the crank wheel surface as shown in Fig. 8(a). In order to consider the influence of the roller diameter, we derived the following compensation equations.

The profile from Eq. (13) is a path of the roller core, thus the actual height of the crank wheel, h' should be changed as

$$h' = h - r_{rol}\cos\alpha \tag{14}$$

and also the phase angle shift at that phase is

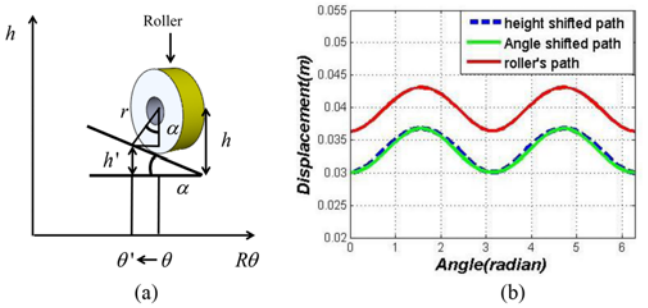

Fig. 8 (a) Kinematic analysis of crank wheel path with considered roller, (b) Design parameter of crank wheel (B: 0.4 Nm, k = 3 N/m r = 6.5 mm)

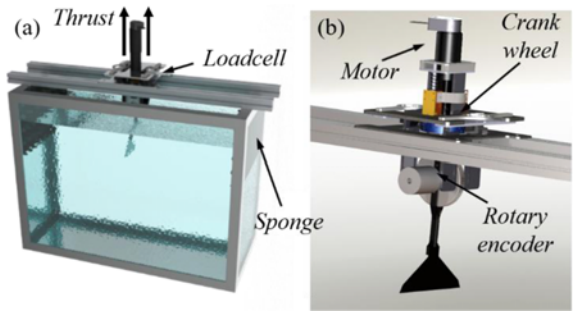

Fig. 9 Illustration of the experimental setup. (a) Water tank with load cell (b) The efficiency-enhanced Scotch yoke mechanism

$$\theta' = \theta - \frac{r_{rol}}{R_C}\sin\alpha \tag{15}$$

where the slope angle α, can be achieved from Eqs. (8) and (11).

In summary, if the spring constant, k and the desired torque amplitude, B is specified, it is possible to generate the surface geometry of the crank wheel. The equations are numerically solved by MATLAB and Fig. 8(b) describes the surface geometry of the crank wheel by considering the influence of the roller when the design data are used. The red solid line is the path of the center of the rollers, the blue dotted line is the path of the shifted height, and the green solid line is the path of the shifted angle.

Table 2 Specification of the apparatus

Water tank	700 mm × 320 mm × 520 mm
Experimental setup	190 mm × 160 mm × 450 mm
Propulsion system mass	1500 g
Compression springs	1.5 N/mm
Motor	Maxon DC Brushes motor (RE35)
Power source	200 W Power supply

Table 3 Torque parameters

Gear ratio	5.8
Maximum current	930 mA
Torque constant	29.2 mNm/A
Maximum torque	29.2 × 0.93 × 5.8 = 0.157 Nm

4. Experimental Evaluation

4.1 Experimental setup

To test the feasibility of the concept, the tests are performed in the apparatus shown in Fig. 9, its specifications of which are listed in Table 2.

Due to the restriction from the size of the water tank, the tail fin is flapped with relatively low frequency. To experiment under this condition, the motor torque is constrained by setting the maximum current of the motor. To decide the maximum torque of the motor, the current is restricted to less than 930 mA and the maximum torque is calculated by the parameters in Table 3.

Based on the maximum torque from Table 3, the crank wheel can be designed. Furthermore, we manufactured the efficiency-enhanced Scotch yoke mechanism by assembling the crank wheel, the springs, and the rollers. We measured the thrust, displacement, current of the motor, and the period of the tail fins. Moreover, we compared between the conventional mechanism and the efficiency-enhanced Scotch yoke mechanism. The experimental setup with two load cells (Ktoyo 333FB) that collects the thrust data is illustrated in Fig. 9(a).

In addition, to prevent the influence of flow, sponges are attached at both sides of the water tank. The tail fin position is measured by the rotary encoder as illustrated in Fig. 9(b). We measured the y-axis thrust using the load cells data recorded at 2000 samples per second with the software LabVIEW installed on the CompactRIO DAQ 9172. Fig. 10(a) shows the crank wheel made according to the design parameters from the equations and Fig. 10(b) shows the rotary encoder, which measures the angle of the tail fin. Twenty carbon fiber sheets of stiffness rigid 907 N/m were used as the tail fin.

4.2 Result analysis

The results of the experiment differ according to the use of the springs. The case where the output torque is regulated by the crank wheel and the springs is denoted by S and the other case is denoted by NS. We assume that the NS case represents a conventional case, since the effect of the shape of the crank wheel on system performance without the spring is negligible. The results between Spring (S) and Non-spring (NS) are compared, while the input current of the motor controller were maintained equal. Table 4 shows the mean value of the thrust and the current for each condition during five cycle of the movement of the tail fin. The thrust is normalized by the period. The result of thrust with springs increased to 27 percent. As a result, the S case has more energy-efficient mechanism than the NS case.

The graphs of the experimental result comparing S and NS are illustrated in Fig. 11. The solid red line describes the S case and the dotted black line shows the NS case. Because the area under the S case graph is bigger than the area of the NS case, the thrust of the S case is higher than the NS case as shown in Fig. 11(a). Fig. 11(b) shows the motion of the tail fin during one cycle. Note that when the tail fin passes the zero flapping angle (from 0.4 s to 0.6 s), the velocity of the NS case decreases sharply since the torque of the motor is insufficient to move the tail fin. Thus, the thrust of the NS case is declined drastically. Contrastively, the S case that had added torque from the springs is able to provide sufficient torque in whole reason.

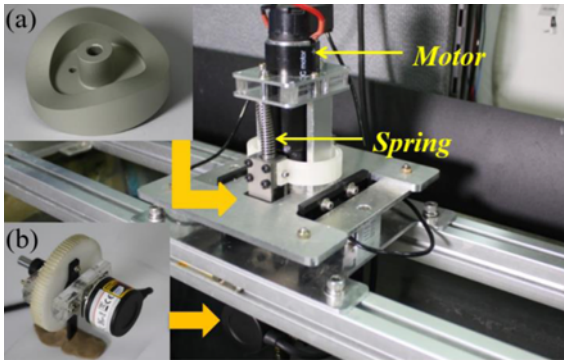

Fig. 10 Experimental setup (a) Crank wheel (b) Rotary encoder (LS mecapion FH40)

Table 4 Experiment result

Condition	Current (± std., mA)	Thrust (± std., mN/s)
NS	925 ± 0.18	475 ± 23
S	925 ± 0.27	606 ± 16

The average thrust of the S case is better than that of the NS case, while the maximum thrust point of the NS case is higher than that of the S case. This phenomenon occurred because the velocity of the NS case is higher than the S case when the tail fin switches direction. It is difficult to increase the velocity of the S case as that of the NS case since the motor is influenced by the compression of the springs. Therefore, the thrust of the NS case increases more than the S case until the velocity of the NS case start to drop. All things considered, the efficiency-enhanced Scotch yoke mechanism is a more efficient method in the propulsion system.

5. Conclusions

The result shows that the efficiency-enhanced Scotch yoke mechanism can increase the thrust by 27 percent within equal motor specification and power consumption. We derived a dynamic model and proposed a method of designing the efficiency-enhanced Scotch yoke mechanism. In addition, we performed experiments to measure the thrust, frequency, and the period of the tail fin movement while the equal input current of the controller is supplied.

The proposed efficiency enhanced scotch yoke mechanism still has room for improvement in the future work. The shape of the crank wheel was designed assuming the largest force is applied when the tail fin passed through the center. However, the required force profile can change depending on the stiffness of the tail fin, and it will determine the optimized shape of the crank wheel. If the crank wheel shape is optimized, the mechanism will provide better results.

The proposed mechanism can be used to make a high-speed robotic fish which requires high thrust force. Additional weight and friction of the equipment needs to be considered for a more accurate estimation of the advantage, but the results show a meaningful increase in the efficiency. In addition, because the basic principle of this mechanism is just transferring a surplus torque to a place where torque is insufficient, it can be applied to various scotch yoke mechanisms with varying required torque such as an electric saw.

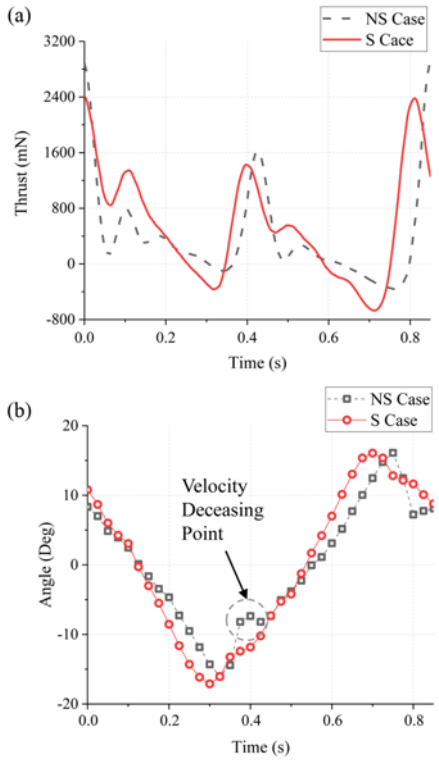

Fig. 11 Graphical synopsis of the experiment result (comparison of the thrust and angular position between S and NS) (a) The thrust result (b) The angle displacement result

ACKNOWLEDGEMENT

This research was supported by ICT R&D program of MSIP/IITP (R0190-15-2040), and Basic Science Research Program through the NRF funded by the Ministry of Education (2014R1A1A2058928).

REFERENCES

1. Liang, J., Wang, T., and Wen, L., "Development of a Two-Joint Robotic Fish for Real-World Exploration," Journal of Field Robotics, Vol. 28, No. 1, pp. 70-79, 2011.

2. Barrett, D. S., "Propulsive Efficiency of a Flexible Hull Underwater Vehicle," Ph.D. Thesis, Massachusetts Institute of Technology, 1996.

3. Hu, H., "Biologically Inspired Design of Autonomous Robotic Fish at Essex," Proc. of IEEE SMC UK-RI Chapter Conference, on Advances in Cybernetic Systems, pp. 3-8, 2006.

4. Zhou, C., and Low, K.-H., "Better Endurance and Load Capacity: An Improved Design of Manta Ray Robot (Roman-II)," Journal of Bionic Engineering, Vol. 7, No. 4, pp. S137-S144, 2010.

5. Yu, J., Su, Z., Wang, M., Tan, M., and Zhang, J., "Control of Yaw and

Pitch Maneuvers of a Multilink Dolphin Robot," IEEE Transactions on Robotics, Vol. 28, No. 2, pp. 318-329, 2012.

6. Cloitre, A., Subramaniam, V., Patrikalakis, N., and y Alvarado, P. V., "Design and Control of a Field Deployable Batoid Robot," Proc. of 4th IEEE RAS & EMBS International Conference on Biomedical Robotics and Biomechatronics (BioRob), pp. 707-712, 2012.
7. Park, Y.-J., Huh, T. M., Park, D., and Cho, K.-J., "Design of a Variable-Stiffness Flapping Mechanism for Maximizing the Thrust of a Bio-Inspired Underwater Robot," Bioinspiration & Biomimetics, Vol. 9, No. 3, Paper No. 036002, 2014.
8. Jeong, S.-K., Choi, H.-S., Bae, J.-H., You, S.-S., Kang, H.S., et al., "Design and Control of High Speed Unmanned Underwater Glider," International Journal of Precision Engineering and Manufacturing-Green Technology, Vol. 3, No. 3, pp. 273-279, 2016.
9. Jun, M. J., Kim, D. H., Choi, H. S., and Han, C. S., "Development of Biomimetic Underwater Vehicle using Single Actuator," Journal of the Korean Society for Precision Engineering, Vol. 33, No. 7, pp. 571-577, 2016.
10. Low, K. H., "Modelling and Parametric Study of Modular Undulating Fin Rays for Fish Robots," Mechanism and Machine Theory, Vol. 44, No. 3, pp. 615-632, 2009.
11. Liu, P., He, K., Ou, X., and Du, R., "Mechanical Design, Kinematic Modeling and Simulation of a Robotic Dolphin," Proc. of IEEE International Conference on Information and Automation (ICIA), pp. 738-743, 2011.
12. Yu, J., Hu, Y., Huo, J., and Wang, L., "Dolphin-Like Propulsive Mechanism Based on an Adjustable Scotch Yoke," Mechanism and Machine Theory, Vol. 44, No. 3, pp. 603-614, 2009.
13. Hu, Y., Wang, L., Yu, J., Huo, J., and Jia, Y., "Development and Control of Dolphin-Like Underwater Vehicle," Proc. of American Control Conference, pp. 2858-2863, 2008.
14. Fan, R., Yu, J., Wang, L., Xie, G., Fang, Y., and Hu, Y., "Optimized sDesign and Implementation of Biomimetic Robotic Dolphin," Proc. of IEEE International Conference on Robotics and Biomimetics (ROBIO, pp. 484-489, 2005.
15. Galiński, C., and Żbikowski, R., "Insect-Like Flapping Wing Mechanism Based on a Double Spherical Scotch Yoke," Journal of the Royal Society Interface, Vol. 2, No. 3, pp. 223-235, 2005.
16. Kim, H. G., Lee, D. G., and Seo, T. W., "Rolling Stability Enhancement Via Balancing Tail for a Water-Running Robot," Journal of Bionic Engineering, Vol. 12, No. 3, pp. 395-405, 2015.
17. Lee, G. J., Kim, J., and Lee, T. S., "The Rolling Scotch Yoke Mechanism Applied to a Small Air Compressor for Oil-Free Operations," International Journal of Precision Engineering and Manufacturing, Vol. 15, No. 1, pp. 97-103, 2014.
18. Yu, J., Li, Y., Hu, Y., and Wang, L., "Towards Development of Link-Based Robotic Dolphin: Experiences and Lessons," Proc. of IEEE International Conference on Robotics and Biomimetics, pp. 240-245, 2009.
19. Park, Y.-J., Jeong, U., Lee, J., Kwon, S.-R., Kim, H.-Y., and Cho, K.-J., "Kinematic Condition for Maximizing the Thrust of a Robotic Fish Using a Compliant Caudal Fin," IEEE Transactions on Robotics, Vol. 28, No. 6, pp. 1216-1227, 2012.

Seok-Ryung Kwon
Researcher in Hyundai Motor Company. His research interests are bio-inspired robotics, novel mechanisms and internal combustion engines.
E-mail: kwons777@snu.ac.kr

Dae-Young Lee
Postdoctoral Fellow of the Soft Robotics Research Center. His research interests are soft robotics, origami inspired mechanism, deployable structure, and smart material.
E-mail: winter2nf@snu.ac.kr

Useok Jeong
Senior researcher in Korea Institute of Industrial Technology (KITECH). His research interests are soft wearable robot, cable driven system, and physical human-robot interaction.
E-mail: usjeong@kitech.re.kr

Yong-Jai Park
Assistant Professor in the Department of Mechatronics Engineering, Kangwon National University. His research interests are soft robotics, bio-inspired robot, novel mechanism, variable stiffness mechanism and soft wearable devices.
E-mail: yjpark@kangwon.ac.kr

Kyu-Jin Cho
Professor of the Mechanical and Aerospace Engineering and the director of the Soft Robotics Research Center, Seoul National University. His research interests include biologically inspired robotics, soft robotics, soft wearable devices, novel mechanisms using smart structures, and rehabilitation and assistive robotics.
E-mail: kjcho@snu.ac.kr